

Production and Equilibration of the Quark-Gluon Plasma with Chromoelectric Field and Minijets

R.S. Bhalerao ^{*} and Gouranga C. Nayak ^{† ‡}

*Department of Theoretical Physics, Tata Institute of Fundamental Research, Homi Bhabha Road,
Colaba, Mumbai 400 005, INDIA*

Abstract

Production and equilibration of quark-gluon plasma are studied within the color flux-tube model, at the RHIC and LHC energies. Non-Abelian relativistic transport equations for quarks, antiquarks and gluons, are solved in the extended phase space which includes coordinates, momenta and color. Before the chromoelectric field is formed, hard and semihard partons are produced via minijets which provide the initial conditions necessary to solve the transport equations. The model predicts that in spite of the vast difference between the RHIC and LHC incident energies, once the local equilibrium is reached, the energy densities, the number densities and the temperatures at the two machines may not be very different from each other. The minijet input significantly alters the evolution of the deconfined matter, unless the color field is too strong. For the input parameters used here the equilibration time is estimated to be ~ 1 fm at RHIC and ~ 0.5 fm at LHC, measured from the instant when the two colliding nuclei have just passed through each other. The temperature at equilibration is found to be ~ 250 MeV at RHIC and ~ 300 MeV at LHC.

PACS numbers: 12.38.Mh, 25.75.-q, 13.87.-a, 24.85.+p

Typeset using REVTeX

^{*}e-mail: bhalerao@theory.tifr.res.in

[†]e-mail: nayak@th.physik.uni-frankfurt.de

[‡]present address: I.T.P., J.W. Goethe-Univ. Frankfurt, Germany

I. INTRODUCTION

Lattice QCD studies indicate that the hadronic matter undergoes a phase transition to the deconfined quark-gluon plasma (QGP) phase, at a sufficiently high temperature ($\simeq 200$ MeV) [1]. The energy density at which this transition is expected to occur is about 2 GeV/fm^3 . Such a phase of deconfined partons did exist in the very early universe and is expected to be created in the laboratory, in ultrarelativistic heavy-ion collisions (URHIC). The Relativistic Heavy-Ion Collider (RHIC) at BNL (Au-Au collisions at $(\sqrt{s})^{NN} = 200$ GeV) and the Large Hadron Collider (LHC) at CERN (Pb-Pb collisions at $(\sqrt{s})^{NN} = 5.5$ TeV) will provide the best opportunity to study the formation of QGP. The main signatures of formation of QGP are sought in (1) J/ψ suppression, (2) strangeness enhancement and (3) dilepton and photon productions [2].

Different stages through which the evolution of deconfined quark-gluon matter proceeds are (1) pre-equilibrium (2) equilibrium and (3) hadronization. While the equilibrium stage is described by the well known hydrodynamic equations [3], it is a difficult problem to study the formation and pre-equilibrium evolution of QGP in URHIC. Nevertheless, the initial conditions which one assumes for the hydrodynamic expansion, can only be determined by a careful study of the pre-equilibrium stage. So it is necessary and important to study the pre-equilibrium stage, which would provide information on the equilibration time, and the bulk properties such as the temperature, the energy density and the number density of QGP. For example, the importance of the correct determination of the equilibration time, in connection with the J/ψ suppression, is stressed by many people [4–6] and it is a challenging task to determine this quantity accurately.

In this paper, we study the pre-equilibrium evolution of QGP within the color flux-tube model. In this model, when two Lorentz-contracted nuclei collide head-on and pass through each other, they acquire a nonzero color charge ($\langle Q \rangle = 0, \langle Q^2 \rangle \neq 0$), by a random exchange of soft gluons. The two receding nuclei act as color capacitor plates and produce a chromoelectric field between them [7,8]. This chromoelectric field causes instability of the QCD vacuum and creates $q\bar{q}$ and gluon pairs via the Schwinger-like mechanism [9–11]. The partons so produced, collide with each other and also get accelerated due to the background field. These color charges also rotate in the color space according to Wong's equation [12]. We consider relativistic non-Abelian transport equations for quarks, antiquarks and gluons. These equations simultaneously include the convective flow terms, the background field acceleration terms, the $q\bar{q}$ and gluon production source terms, the collision terms and the terms which take into account rotations of these color charges due to the background chromoelectric field. We solve these transport equations together with the Yang-Mills equations.

As mentioned above, the initial chromoelectric field owes its existence to nonperturbative processes, viz., the soft-gluon exchanges that take place between the two nuclei during the collision. This model describes mostly the production of soft partons [13,14]. As pointed out in [15] and also in [14], the (semi)hard processes (via perturbative QCD) take place before the soft-gluon exchanges. By adding these hard processes to the color flux-tube model, *we attempt to cover the full range of particle production mechanisms, thereby including both soft and hard partons in the evolution of the deconfined parton matter.* It has been shown by several authors that minijet production is dominant in the very early stages of the collision of two nuclei at the RHIC and LHC energies [16]. Earlier studies [17,13,14] of the

pre-equilibrium domain ignored the minijets. In this paper, we have calculated the minijet production at RHIC and LHC and have combined it with the color flux-tube model to study the production and evolution of QGP. A similar attempt was made by Eskola and Gyulassy [15] within the hydrodynamics framework which is applicable only *after* local equilibrium is attained. Here we study the *pre-equilibrium* evolution by solving relativistic non-Abelian transport equations with both the hard and soft partons taken into account. *We address ourselves to the important question whether QGP, if formed, would attain substantially higher temperatures at LHC than at RHIC.* We also investigate relative importance of the hard and soft production mechanisms.

The plan of the paper is as follows. In section II, we describe our model with a detailed discussion of minijet production and of transport equations with their analytic solutions. Here we also present our computational procedure. In section III, we describe our numerical results and discuss them. We then compare our model with some other models of the early evolution of the matter in URHIC. Finally in section IV, we present our conclusions.

II. MODEL

In our model, all hard and semihard partons (i.e., minijets) are formed before the chromoelectric field is created due to the exchange of soft gluons. In all earlier studies of pre-equilibrium evolution of QGP within the color flux-tube model [17,13,14], there was only the background field and no particles, at the initial time. In other words, the initial particle distribution functions were taken to be zero in all these calculations. In the present work, we obtain the initial particle distributions from minijets. With this initial condition, we then solve the transport equations at the RHIC and LHC energies. Our aim is to study the possible effect of the minijets on the equilibration process.

The relativistic non-Abelian transport equations which we want to solve are presented in [18,14], in detail. In order to include the color charge in the phase space, one considers an extended one-particle phase space of dimension $d = 6 + (N^2 - 1)$, (with $N = 3$). The extended phase space is taken to be the direct sum $R^6 \oplus G$, where G is the (compact) space corresponding to the given gauge group. Thus, in addition to the usual 3 space coordinates and 3 momentum coordinates, one now has 8 coordinates corresponding to the 8 color charges in SU(3). In this extended phase space, a typical transport equation in the notation of [18], reads as

$$\left[p_\mu \partial^\mu + g Q^a F_{\mu\nu}^a p^\nu \partial_p^\mu + g f^{abc} Q^a A_\mu^b p^\mu \partial_Q^c \right] f(x, p, Q) = C(x, p, Q) + S(x, p, Q). \quad (1)$$

Here $f(x, p, Q)$ is the single-particle distribution function in the extended phase space. The first term on the LHS of Eq. (1) corresponds to the usual convective flow, the second term is the non-Abelian version of the Lorentz force term and the third term corresponds to the precession of the color charge, as described by Wong's equation [12]. C and S on the RHS of Eq. (1) are the collision and the source terms, respectively. Note that there are separate transport equations for quarks, antiquarks and gluons [18].

In order to solve the transport equations, we need the initial distribution functions f_0 , which we now obtain using minijet production cross sections.

A. Minijet production at RHIC and LHC

Hard and semihard partons expected to be produced at RHIC and LHC are mostly minijets whose average momenta are not very large. One can calculate the minijet cross sections after fixing a momentum scale (p_T) above which perturbative QCD (pQCD) is applicable. In the lowest order pQCD the inclusive ($2 \rightarrow 2$) minijet cross section per nucleon in AA collision is given by [15,16]

$$\sigma_{jet} = \int dp_T dy_1 dy_2 \frac{2\pi p_T}{\hat{s}} \sum_{ijkl} x_1 f_{i/A}(x_1, p_T^2) x_2 f_{j/A}(x_2, p_T^2) \hat{\sigma}_{ij \rightarrow kl}(\hat{s}, \hat{t}, \hat{u}). \quad (2)$$

Here x_1 and x_2 are the light-cone momentum fractions carried by the partons i and j from the projectile and the target, respectively, f are the bound-nucleon structure functions and y_1 and y_2 are the rapidities of the scattered partons. The symbols with carets refer to the parton-parton c.m. system. The $\hat{\sigma}_{ij \rightarrow kl}$ is the elementary pQCD parton cross section. The required $\hat{\sigma}_{ij \rightarrow kl}$ are given by

$$\hat{\sigma}_{qq' \rightarrow qq'} = \frac{4\alpha_s^2}{9\hat{s}} \left[\frac{\hat{s}^2 + \hat{u}^2}{\hat{t}^2} \right], \quad (3)$$

$$\hat{\sigma}_{q\bar{q} \rightarrow q'\bar{q}'} = \frac{4\alpha_s^2}{9\hat{s}} \left[\frac{\hat{t}^2 + \hat{u}^2}{\hat{s}^2} \right], \quad (4)$$

$$\hat{\sigma}_{qq \rightarrow qq} = \frac{4\alpha_s^2}{9\hat{s}} \left[\frac{\hat{s}^2 + \hat{u}^2}{\hat{t}^2} + \frac{\hat{s}^2 + \hat{t}^2}{\hat{u}^2} - \frac{2\hat{s}^2}{3\hat{t}\hat{u}} \right], \quad (5)$$

$$\hat{\sigma}_{q\bar{q} \rightarrow q\bar{q}} = \frac{4\alpha_s^2}{9\hat{s}} \left[\frac{\hat{s}^2 + \hat{u}^2}{\hat{t}^2} + \frac{\hat{t}^2 + \hat{u}^2}{\hat{s}^2} - \frac{2\hat{u}^2}{3\hat{s}\hat{t}} \right], \quad (6)$$

$$\hat{\sigma}_{q\bar{q} \rightarrow gg} = \frac{8\alpha_s^2}{3\hat{s}} (\hat{t}^2 + \hat{u}^2) \left[\frac{4}{9\hat{t}\hat{u}} - \frac{1}{\hat{s}^2} \right], \quad (7)$$

$$\hat{\sigma}_{gg \rightarrow q\bar{q}} = \frac{3\alpha_s^2}{8\hat{s}} (\hat{t}^2 + \hat{u}^2) \left[\frac{4}{9\hat{t}\hat{u}} - \frac{1}{\hat{s}^2} \right], \quad (8)$$

$$\hat{\sigma}_{gq \rightarrow gq} = \frac{\alpha_s^2}{\hat{s}} (\hat{s}^2 + \hat{u}^2) \left[\frac{1}{\hat{t}^2} - \frac{4}{9\hat{s}\hat{u}} \right], \quad (9)$$

$$\hat{\sigma}_{gg \rightarrow gg} = \frac{9\alpha_s^2}{2\hat{s}} \left[3 - \frac{\hat{u}\hat{t}}{\hat{s}^2} - \frac{\hat{u}\hat{s}}{\hat{t}^2} - \frac{\hat{s}\hat{t}}{\hat{u}^2} \right]. \quad (10)$$

Here α_s is the strong coupling constant, q and q' denote distinct flavors of quark, and

$$\hat{s} = x_1 x_2 s = 4p_T^2 \cosh^2 \left(\frac{y_1 - y_2}{2} \right). \quad (11)$$

The rapidities y_1 , y_2 and the momentum fractions x_1 , x_2 are related by,

$$x_1 = p_T (e^{y_1} + e^{y_2})/\sqrt{s}, \quad x_2 = p_T (e^{-y_1} + e^{-y_2})/\sqrt{s}. \quad (12)$$

The limits of integrations of rapidities y_1 and y_2 are given by, $|y_1| \leq \ln(\sqrt{s}/2p_T + \sqrt{s/4p_T^2 - 1})$ and $-\ln(\sqrt{s}/p_T - e^{-y_1}) \leq y_2 \leq \ln(\sqrt{s}/p_T - e^{y_1})$. We multiply the above minijet cross sections by the well known factor $K = 2$, to account for the $O(\alpha_s^3)$ contributions.

The structure functions $f_{i,j/A}$ occurring in Eq. (2) are obtained from the model of Eskola *et al.* [19,20], and using the GRV HO 94 set of parton distributions for a free nucleon.

As argued in [15], we choose minimum $p_T = 2$ GeV, above which pQCD is assumed to be applicable.

B. Initial conditions for plasma evolution from minijets

For central collisions, the minijet cross section (Eq. (2)) can be related to the total number of partons (N) by

$$N = T(0) \sigma_{jet}, \quad (13)$$

where $T(0) = 9A^2/8\pi R_A^2$ is the nuclear geometrical factor for head-on AA collisions (for a nucleus with a sharp surface) [16]. Here $R_A = 1.2A^{1/3}$ is the nuclear radius. The total transverse energy $\langle E_T^{tot} \rangle$ produced in nuclear collisions, from minijets, can be shown to be

$$\langle E_T^{tot} \rangle = T(0) \int dp_T p_T dy_1 dy_2 \frac{2\pi p_T}{\hat{s}} \sum_{ijkl} x_1 f_{i/A}(x_1, p_T^2) x_2 f_{j/A}(x_2, p_T^2) \hat{\sigma}_{ij \rightarrow kl}(\hat{s}, \hat{t}, \hat{u}). \quad (14)$$

We will use these relations (Eqs. (2), (13) and (14)) to determine the initial conditions which are required to solve the transport equations (Eq. (1)) in the pre-equilibrium stage.

In the color flux-tube model, we assume that the chromoelectric field is formed when the two nuclei completely pass through each other. The volume of the system at that instant is $V_0 = \pi R_A^2 d$, where d is the longitudinal thickness of the system. Note that d depends on the incident energy because of the Lorentz contraction and the presence of the wee partons in the incoming nuclei. We have taken $d = 3$ fm at RHIC for Au-Au collisions and $d = 2$ fm at LHC for Pb-Pb collisions [21]. Using (Eqs. (2), (13) and (14)), we calculate the initial number density (n_0), initial energy density (ϵ_0) and initial distribution functions (f_0) of quarks, antiquarks and gluons, which are needed to solve the transport equations. These are $n_0 = N/V_0$, $\epsilon_0 = \langle E_T^{tot} \rangle / V_0$ and $f_0 = dn_0/d^3p$. Here

$$d^3p = d^2 p_T dp_z = p_T d^2 p_T \cosh y_1 dy_1, \quad (15)$$

and f_0 can be easily extracted from Eq. (13) with the help of Eqs. (2) and (15).

In Table I we present our results for the initial conditions, obtained from minijet production at RHIC and LHC.

C. Solution of the relativistic transport equations

In order to solve the transport equations (1), we need to specify the collision and the source terms occurring on the RHS.

We measure the proper time τ from the instant the two colliding nuclei have just passed through each other. In our model, hard partons (in the form of the minijets) are present in the system at $\tau = 0$ and soft partons are created by the background field at later times. It is not possible to obtain the collision term from pQCD alone because the latter provides a framework to treat only the *hard* collisions; collisions among *soft* partons cannot be handled by pQCD. Including the effects of soft collisions, in the transport equations (1), from first principles (QCD) is a difficult problem. We make the relaxation-time approximation to simulate the effects of both soft and hard collisions and write the collision term as:

$$C = -p^\mu u_\mu (f - f^{eq})/\tau_c, \quad (16)$$

where u^μ is the four velocity, f^{eq} is the equilibrium distribution function (Fermi-Dirac for quarks and antiquarks, and Bose-Einstein for gluons) and τ_c is the relaxation time. We take the same expressions for the source terms (S) as in [14].

Following Bjorken's proposal [3], we express all physical observables in terms of the boost invariant quantities, namely

$$\tau = (t^2 - z^2)^{1/2}, \quad \xi = \eta - y, \quad p_T = (p_0^2 - p_l^2)^{1/2}, \quad (17)$$

where $\eta = \tanh^{-1}(z/t)$ is the space-time rapidity and $y = \tanh^{-1}(p_l/p_0)$ is the momentum rapidity. The transport equations (1) can be rewritten in terms of these variables.

The formal solutions of the transport equations can be found to be,

$$\begin{aligned} f_{q,\bar{q},g}(\tau, \xi, p_T, Q) &= \int_0^\tau d\tau' \exp\left(\frac{\tau' - \tau}{\tau_c}\right) \left[\frac{S_{q,\bar{q},g}(\tau', \xi', p_T, Q)}{p_T \cosh \xi'} + \frac{f_{q,\bar{q},g}^{eq}(\tau', \xi', p_T, Q)}{\tau_c} \right] \\ &+ \exp(-\tau/\tau_c) f_0^{q,\bar{q},g}, \end{aligned} \quad (18)$$

where ξ' is given by

$$\xi' = \sinh^{-1} \left[\frac{\tau}{\tau'} \sinh \xi + \frac{g \cos \theta_1}{p_T \tau'} \int_{\tau'}^\tau d\tau'' \tau'' E(\tau'') \right], \quad (19)$$

and $f_0^{q,\bar{q},g}$ are the initial distribution functions of quarks, antiquarks and gluons obtained from minijets (as described in subsections IIA-B). The initial distribution function was assumed to be zero in all earlier studies of the color flux-tube model [17,13,14]. In the above equation, θ_1 is the angle between the chromoelectric field and the color charge in the SU(3) color space [14].

Since both the field and the particles are present simultaneously, we use the following relation for the conservation of the energy-momentum tensor:

$$\partial_\mu T_{mat}^{\mu\nu} + \partial_\mu T_f^{\mu\nu} = 0. \quad (20)$$

Here

$$T_{mat}^{\mu\nu} = \int p^\mu p^\nu (3f_q + 3f_{\bar{q}} + f_g) d\Gamma d\Omega, \quad (21)$$

and

$$T_f^{\mu\nu} = \text{diag}(E^2/2; E^2/2, E^2/2, -E^2/2). \quad (22)$$

In Eq. (21), the factor 3 refers to the three flavors of quarks, $d\Gamma = d^3p/(2\pi)^3 p_0 = p_T dp_T d\xi/(2\pi)^2$, and $d\Omega$ is the angular integral measure in the color space. We follow the same procedure as in [14,17] and finally obtain the evolution equation for the field as:

$$\frac{dE(\tau)}{d\tau} - \frac{g}{(2\pi)^2} \int_0^\infty dp_T p_T^2 \int_{-\infty}^\infty d\xi \sinh \xi \int d\Omega [3f_q - 3f_{\bar{q}} + f_g] + (\pi^3/6)\bar{a}|E(\tau)|^{3/2} = 0. \quad (23)$$

Here $\bar{a} = a\zeta(5/2) \exp(0.25/\alpha)$, $a = c(g/2)^{5/2} \frac{9}{2(2\pi)^3}$, $c = \frac{2.876}{4\pi^3}$ and $\zeta(5/2) = 1.342$ is the Riemann zeta function.

To solve Eq. (23), we fix the form of the local temperature $T(\tau)$, by demanding that the particle energy density $\epsilon_p(\tau)$ at any instant, differs negligibly from the equilibrium energy density at temperature $T(\tau)$ at that instant. (It may be noted that $T(\tau)$ occurs in Eq. (18) and hence in Eq. (23), through f^{eq} .) This allows us to write the temperature $T(\tau)$ in terms of the particle energy density $\epsilon_p(\tau)$ as follows

$$T(\tau) = \left[\frac{36\epsilon_p(\tau)}{5\pi^6} \right]^{1/4}, \quad (24)$$

where

$$\epsilon_p(\tau) = \int d\Gamma d\Omega (p^\mu u_\mu)^2 (3f_q + 3f_{\bar{q}} + f_g). \quad (25)$$

We solve Eq. (23) numerically to study time evolution of the chromoelectric field.

Finally, the number density of the quark-gluon matter is given by

$$n(\tau) = \int d\Gamma d\Omega p^\mu u_\mu (3f_q + 3f_{\bar{q}} + f_g). \quad (26)$$

D. Computational procedure

In the present work, we have determined $E(\tau)$ and $T(\tau)$ by imposing the following double self-consistency requirement. Starting with trial $E(\tau)$ and $T(\tau)$ and using Eqs. (18) we determine f_q , $f_{\bar{q}}$ and f_g . These when substituted in Eq. (25) give us $\epsilon_p(\tau)$ which in turn gives a new temperature $T(\tau)$ by Eq. (24). The new $T(\tau)$ and the trial $E(\tau)$ are again used in Eqs. (18), and with the new f_q , $f_{\bar{q}}$ and f_g thus determined, the differential equation (23) is solved to get a new field $E(\tau)$. This process is iterated until convergence is reached. This gives us a self-consistent set of $E(\tau)$, $T(\tau)$, $\epsilon_p(\tau)$, f_q , $f_{\bar{q}}$ and f_g .

III. RESULTS AND DISCUSSION

With the minijet initial conditions, we solve the transport equations (1) from the instant the two wounded nuclei have just crossed each other up to $\tau \simeq 1.5$ fm. The solution of the transport equations allows us to determine the time evolution of the physical quantities such as energy density, number density and temperature. The determination of these quantities is important for the prediction of any signature of quark-gluon plasma. We now present our numerical results for these quantities. As in [14], we take $g = 4$ and $\tau_c = 0.2$ fm. For the initial field energy density $\epsilon_f(0)$, we take either 0 or 300 GeV/fm³. This allows us to discuss the following three scenarios: (a) vanishing field, (b) $\epsilon_f(0)$ comparable to the initial minijet energy density ϵ_0 , and (c) $\epsilon_f(0) \gg \epsilon_0$. Thus we can study the effect of the variation of the initial field on the calculated results.

In all the figures, $\tau = 0$ corresponds to the instant when the two colliding nuclei have just passed through each other, and $\epsilon_f(0) = 300$ GeV/fm³ unless stated otherwise.

In Fig. 1, we have presented the parton energy densities for RHIC and LHC. It can be seen that the evolution of the parton energy density with minijet inputs at RHIC, is almost the same as that without the minijet inputs (dashed curve). This is because, at RHIC, the initial minijet energy density ϵ_0 ($\simeq 3$ GeV/fm³) is negligible compared to $\epsilon_f(0)$; see Table I. At LHC, the two results are different because ϵ_0 ($\simeq 178$ GeV/fm³) is comparable to $\epsilon_f(0)$. *Thus the inclusion of the minijet input substantially alters the evolution of the parton energy density unless the chromoelectric field is too strong.*

We now discuss qualitatively the shapes of the curves in Fig. 1. It is easy to see from Eq. (18) that the parton energy density evolves as

$$\epsilon_p(\tau) = \epsilon(\tau) + e^{-\tau/\tau_c} \epsilon_0. \quad (27)$$

Here, $\epsilon(\tau)$ is the energy density if there is no minijet production, i.e., if the particle production is only from the field. The decrease in the energy density at earlier times (see the curve labelled LHC in Fig. 1) is due to the multiplicative factor $e^{-\tau/\tau_c}$ occurring in Eq. (27). The further increase in the energy density is due to the fact that the particle production from the field starts dominating by this time (this is $\epsilon(\tau)$ in Eq. (27)). We shall show below that the fall in the energy density after it reaches the maximum value is close to what is expected if the system has attained a local equilibrium and is expanding according to the hydrodynamic equations. Then it is clear from Fig. 1 that *the equilibration of plasma is expected to occur earlier and the temperature at equilibration is expected to be somewhat higher at LHC*. This will have a significant effect on all the predictions of QGP signatures.

In Fig. 2, we compare the evolution of the parton energy density, at LHC, with and without the background field. This is necessary because the initial strength of the field cannot be calculated easily and as the incident energy increases the possibility of soft-gluon exchanges may become small. So we have presented our results for the two extreme cases (1) vanishing field energy density and (2) a very high initial field energy density (300 GeV/fm³). The actual results are expected to fall within these two limits. Qualitatively similar results are expected at the RHIC energy too.

Thus the background field representing the collective long-range effects plays an important role in the evolution of the system. If the minijet initial conditions based on pQCD are to play an important role at RHIC, then the field will have to be about two orders

of magnitude weaker than what we have assumed. In other words, if at RHIC, the initial field energy density $\epsilon_f(0)$ was not $300 \text{ GeV}/\text{fm}^3$, but only $3 \text{ GeV}/\text{fm}^3$, then $\epsilon_f(0)$ would be comparable to the initial minijet energy density $\epsilon_0(\text{RHIC}) \simeq 3 \text{ GeV}/\text{fm}^3$, and results qualitatively similar to those shown in Fig. 2 would be obtained at the RHIC energy too. In the HIJING [22] and Parton Cascade models [21], the background field was completely neglected.

Comparison of the two curves labelled ‘Field’ and ‘Field+Minijets’, in Fig (2), shows the effect of the minijets on $\epsilon_p(\tau)$. The memory of the minijet input is nearly wiped out at large τ because of the exponential decay factor in Eq. (27). *As a result, the large kinetic energy of the two colliding nuclei at LHC may not necessarily translate into large temperature of the equilibrated deconfined matter.* Actual calculation shows that the temperature when the equilibrium is reached is $\sim 300 \text{ MeV}$ at LHC and $\sim 250 \text{ MeV}$ at RHIC, *not very different from each other.* Comparison of the two curves labelled ‘Minijets’ and ‘Field+Minijets’ shows the effect of the field on $\epsilon_p(\tau)$; this effect survives till relatively larger τ . Note also that *if there is no background field, the $\epsilon_p(\tau)$ decreases monotonically.*

The decay of the chromoelectric field is shown in Fig. 3. The decay is much faster at LHC than at RHIC, again suggesting an early equilibration at LHC. The evolution of the field strength has a significant impact on the acceleration of partons. If the chromoelectric field survives even after local equilibrium is reached, then the subsequent evolution of the system is governed by the chromoviscous hydrodynamic equations [15], instead of Bjorken’s hydrodynamic equations [3]. So it is very important to study the evolution of the chromoelectric field in the pre-equilibrium stage. *We find that the equilibration time of the deconfined matter and the life-time of the field are nearly the same.*

In Fig. 4, we have presented the parton number densities of the system, for both the RHIC and LHC energies. The behavior of the results is the same as that of the parton energy densities in Fig. 1, because an equation similar to Eq. (27) holds for the number density too. The maximum number density at LHC is $\sim 120 \text{ fm}^{-3}$, whereas at RHIC it is $\sim 90 \text{ fm}^{-3}$. *However, at large τ , when the systems have equilibrated, the two number densities are nearly the same.* These partons produce/affect all the signatures of QGP and hence their evolution plays a crucial role in QGP detection.

We have fitted $\epsilon_p(\tau)$, $n(\tau)$ and $T(\tau)$, for $\tau \geq 0.5 \text{ fm}$, at the LHC energy, with a functional form $a\tau^{-b}$, where a and b are constants. We find that $b = 1.23, 0.70$ and 0.31 , respectively. According to Bjorken’s hydrodynamics, these values are $1.33, 1$ and 0.33 , respectively. Comparing these two sets of values with each other, we conclude that the system has nearly equilibrated at $\tau \simeq 0.5 \text{ fm}$, at LHC. Similarly, at RHIC, the equilibration time is found to be $\simeq 1 \text{ fm}$. Recall that these time intervals are measured from the instant when the two colliding nuclei have just passed through each other.

In Figs. 5 and 6, we have presented our results for the number densities of quarks plus antiquarks and gluons, respectively. Consider the curves labelled LHC in these two figures. The initial number density in Fig. 5 is much less than that in Fig. 6, because the minijet gluon production is much larger; see Eqs. (3)-(10). In Fig. 5, initially, the number density increases with time because of the large production of q and \bar{q} from the field; see Eq. (26) which receives a separate contribution from each of the 3 flavors of quarks and antiquarks. Although the gluon production is 1.5 times more likely than that of quarks via the Schwinger-like mechanism [11], the counting in Eq. (26) eventually builds up a larger

quark plus antiquark density than the gluon density. In Fig. 6, the LHC number density decreases with time because of the dominance of the exponential factor $\exp(-\tau/\tau_c)$ in Eq. (18), over the gluon production by the field. The energy densities for quarks plus antiquarks and gluons are plotted in Figs. 7 and 8, respectively. The behavior remains the same as in Figs. 5 and 6.

We now compare our model with some well known models of the early stages of the ultra-relativistic heavy-ion collisions, namely the parton cascade model (PCM) [21], the HIJING model [22], the McLerran-Venugopalan model (MVM) [23], etc.

As is well known, PCM is a pQCD-based model. It neglects the long-range collective effects which we have attempted to incorporate here by means of a background field. The PCM starts by defining a classical phase-space distribution function for the two incoming nuclei, which is then evolved by means of the Boltzmann equation retaining only the convective-flow term and the collision term in Eq. (1). Now it is known that there are wee partons in each of the two nuclei and each wee parton spreads over the entire width of the nucleus [24]. It is difficult to define a classical distribution function for such a system of particles. Indeed the incoming nuclei are in pure quantum mechanical states. Hence solving the classical transport equation right from the instant the two incoming nuclei start touching each other, is a questionable procedure.

A classical distribution function can be more justifiably defined when the spatial extent and the time intervals are larger than the average de Broglie wave length of the partons. In our model, we have started the classical evolution at a time when the two nuclei have completely crossed each other. At that instant, in our model, there are only hard partons ($p_T > 2 \text{ GeV}/c$); the soft partons are created later when the system has grown even bigger. The initial condition for the hard part is obtained via the minijet calculation where no approximation is involved. The initial condition for the soft part is taken through the creation of a coherent chromoelectric field.

The HIJING model too is a pQCD-based model. It combines pQCD processes with string phenomenology for non-perturbative soft processes. It *assumes* that the parton distributions can be approximated by thermal phase-space distributions with non-equilibrium fugacities. Thus the issue of thermalization of the deconfined matter in the framework of the kinetic theory is not addressed.

Thus we have presented a model which is different from PCM and the HIJING Model. We believe that this model has some desirable features. For simplicity, we have neglected the interactions among the minijets before $\tau = 0$. Our main aim has been to see how the minijet input modifies our earlier analysis [14]. It will be interesting to consider these interactions. Although pQCD provides a general framework for this purpose, including these interactions is quite nontrivial.

Our approach has some similarities with the McLerran-Venugopalan model. The MVM is a classical effective field theory description of the small- x modes in very large nuclei at very high energies. This effective theory contains a scale μ which is proportional to the large gluon density at small x . The large gluon density ensures that even if the coupling is weak, the fields may be highly nonperturbative. They argued that the classical fields corresponding to the saddle point solutions of the effective theory are the non-Abelian analogue of the Weizsäcker-Williams fields in classical electrodynamics. Now in a collision of such Weizsäcker-Williams fields, the production of incoherent partons with transverse momenta $p_T \gg \alpha_s \mu$ can be

handled by means of pQCD and their propagation in the coherent field can be studied with the help of a classical transport equation [25]. In our model too both incoherent hard partons and coherent field (soft part) are taken into account. So in this sense our approach is similar to MVM.

Real-time simulation of the full, nonperturbative evolution of the classical non-Abelian Weizsäcker-Williams fields on lattice, for the gauge group $SU(2)$, has recently been studied by Krasnitz and Venugopalan [26]; see also [27]. The calculation in [26] incorporates coherence effects which become important at small x and small p_T , while reproducing simultaneously the standard minijet results at large p_T . However, the important issue of equilibration of gluons was not addressed. It will also be interesting to see both the coherent field and incoherent partons simultaneously taken into account in such a simulation.

IV. CONCLUSIONS AND FUTURE PROSPECTS

We have studied the production and equilibration of the quark-gluon plasma expected to be formed in ultrarelativistic heavy-ion collisions, at RHIC and LHC, within the color flux-tube model. The distribution functions of quarks, antiquarks and gluons are defined in the extended phase space of dimension 14 in $SU(3)$. We have solved the non-Abelian relativistic transport equations for these distribution functions. The quarks, antiquarks and gluons are produced from the background field which is formed due to soft-gluon exchanges, via the Schwinger-like mechanism. The initial distribution functions of partons are calculated from the minijet production at RHIC and LHC.

The model predicts that

- (i) The inclusion of the minijet input substantially alters the evolution of the bulk properties of the deconfined matter unless the chromoelectric field is too strong.
- (ii) Equilibration of the deconfined matter is expected to be faster at LHC than at RHIC. Estimated equilibration times are given.
- (iii) Surprisingly, in spite of the large difference between the LHC and RHIC colliding beam energies, the differences between the temperatures and equilibrium energy and number densities attained at the two machines, may not be very large. This is because the memory of the minijet input decays exponentially with time. Estimated numerical values for these physical quantities are given.
- (iv) Unlike the minijets, the effect of the background field survives over a longer time.
- (v) In the absence of a background field, the parton energy density and the number density decrease monotonically with time.
- (vi) The equilibration time of the deconfined matter and the life-time of the chromoelectric field are nearly the same.

In summary, we have combined the non-perturbative aspects of QGP (background chromoelectric field formation) with the perturbative aspects (minijet production) and have studied the evolution of the quark-gluon plasma.

We have used in this work the Schwinger-like source terms [9–11] for parton production from a chromoelectric field. This mechanism is strictly applicable only for a constant, uniform field. However, in a heavy-ion collision, as the system evolves, the field acquires space-time dependence. Particle production in such a field has been studied and an appro-

priate source term has been derived in [28], which will be incorporated in the pre-equilibrium evolution of the QGP and results will be reported elsewhere.

Note added:

Recently Bloch et al. have studied the thermodynamics of strong-field plasmas [29]. In the present paper, we used a classical transport equation while they have used a quantum equation. Our equation is non-Abelian, theirs is Abelian. Our initial conditions are different from theirs. Our source term is also different from theirs. But still the time dependence of the various quantities (their Figs. 1-3) is qualitatively similar to that obtained by us. This shows the robustness of our findings.

ACKNOWLEDGMENTS

We thank R.V. Gavai for many useful discussions.

REFERENCES

- [1] A. Polyakov, Phys. Lett. B **72**, 477 (1978); L. Susskind, Phys. Rev. D **20**, 2610 (1979); C. Borgs and E. Seiler, Nucl. Phys. B **215** [FS7], 125 (1983); Comm. Math. Phys. **91**, 329 (1983). For the status of the lattice QCD, see Proc. of the 17th Intl. Sympo. on Lattice Field Theory (Lattice'99), Pisa, Italy, June-July 1999, to appear in Nucl. Phys. B (Proc. Suppl.).
- [2] For the status of the various signatures, see the Proc. of the 14th Intl. Conf. on Ultra-relativistic Nucleus-Nucleus Collisions (QM'99), Torino, Italy, May 1999, to appear in Nucl. Phys. A.
- [3] J.D. Bjorken, Phys. Rev. D **27**, 140 (1983).
- [4] G.C. Nayak, JHEP **02** (1998) 005.
- [5] G.C. Nayak, Phys. Lett. B **442**, 427 (1998).
- [6] X.-M. Xu, D. Kharzeev, H. Satz and X.-N. Wang, Phys. Rev. C **53**, 3051 (1996).
- [7] F.E. Low, Phys. Rev. D **12**, 163 (1975).
- [8] S. Nussinov, Phys. Rev. Lett. **34**, 1286 (1975).
- [9] J. Schwinger, Phys. Rev. **82**, 664 (1951).
- [10] A. Casher, H. Neuberger and S. Nussinov, Phys. Rev. D **20**, 179 (1979).
- [11] M. Gyulassy and A. Iwazaki, Phys. Lett. B **165**, 157 (1985).
- [12] S.K. Wong, Nuovo Cimento A **65**, 689 (1970).
- [13] G.C. Nayak and V. Ravishankar, Phys. Rev. D **55**, 6877 (1997).
- [14] G.C. Nayak and V. Ravishankar, Phys. Rev. C **58**, 356 (1998).
- [15] K.J. Eskola and M. Gyulassy, Phys. Rev. C **47**, 2329 (1993).
- [16] K.J. Eskola, K. Kajantie and J. Lindfors, Nucl. Phys. B **323**, 37 (1989); K.J. Eskola and K. Kajantie, Z. Phys. C **75**, 515 (1997); X.-N. Wang, Phys. Rev. D **43**, 104 (1991).
- [17] K. Kajantie and T. Matsui, Phys. Lett. B **164**, 373 (1985); B. Banerjee, R.S. Bhalerao and V. Ravishankar, Phys. Lett. B **224**, 16 (1989); A. Bialas, W. Czyz, A. Dyrek and W. Florkowski, Nucl. Phys. B **296**, 611 (1988).
- [18] H.-T. Elze and U. Heinz, Phys. Rep. **183**, 81 (1989).
- [19] K.J. Eskola, V.J. Kolhinen and P.V. Ruuskanen, Nucl. Phys. B **535**, 351 (1998).
- [20] K.J. Eskola, V.J. Kolhinen and C.A. Salgado, e-print hep-ph/9807297.
- [21] K. Geiger, Phys. Rep. **258**, 237 (1995).
- [22] X.-N. Wang, Phys. Rep. **280**, 287 (1997).
- [23] L. McLerran and R. Venugopalan, Phys. Rev. D **49**, 2233 (1994); D **49**, 3352 (1994).
- [24] J.D. Bjorken in Current Induced Reactions: Proc. of the 7th Intl. Summer Inst. on Theoretical Particle Physics, Hamburg 1975, edited by J.G. Körner, G. Kramer and D. Schildknecht, Springer-Verlag, Berlin, 1976, (Lecture Notes in Physics, Vol. 56), page 93; J.D. Bjorken in Proc. of the Summer Inst. on Particle Physics, Stanford, July 1973, edited by D.W.G.S. Leith and S.D. Drell, Vol. 1, page 1.
- [25] L. McLerran, private communication.
- [26] A. Krasnitz and R. Venugopalan, Nucl. Phys. B **557**, 237 (1999).
- [27] W. Poeschl and B. Mueller Phys. Rev. D **60**, 114505 (1999); S.A. Bass, B. Mueller and W. Poeschl, J. Phys. G **25**, L109 (1999); A. Kovner, L. McLerran and H. Weigert, Phys. Rev. D **52**, 3809 (1995); D **52**, 6231 (1995).
- [28] R.S. Bhalerao and V. Ravishankar, Phys. Lett. B **409**, 38 (1997).
- [29] J.C.R. Bloch, C.D. Roberts and S.M. Schmidt, e-print nucl-th/9910073.

TABLE I. Initial conditions for pre-equilibrium evolution of QGP, obtained from the minijet calculation.

	$(\sqrt{s})^{NN}$ (GeV)	N	V_0 (fm ³)	n_0 (fm ⁻³)	ϵ_0 (GeV/fm ³)
RHIC	200	504	459	1.1	3
LHC	5500	17422	318	55	178

Figure captions

FIG. 1. Parton energy density vs proper time. The dashed line refers to the calculation without the minijets.

FIG. 2. Parton energy density vs proper time, at the LHC energy. The curve labelled Field (Minijets) is based on the calculation without the minijets (background field). The curve labelled Field + Minijets is based on the full calculation with both the minijets and the background field taken into account.

FIG. 3. Chromoelectric field vs proper time. The dashed line as in Fig. 1.

FIG. 4. Number density vs proper time. The dashed line as in Fig. 1.

FIG. 5. Number density for quarks and antiquarks vs proper time. The dashed line as in Fig. 1.

FIG. 6. Number density for gluons vs proper time. The dashed line as in Fig. 1.

FIG. 7. Energy density for quarks and antiquarks vs proper time. The dashed line as in Fig. 1.

FIG. 8. Energy density for gluons vs proper time. The dashed line as in Fig. 1.

Fig. 1

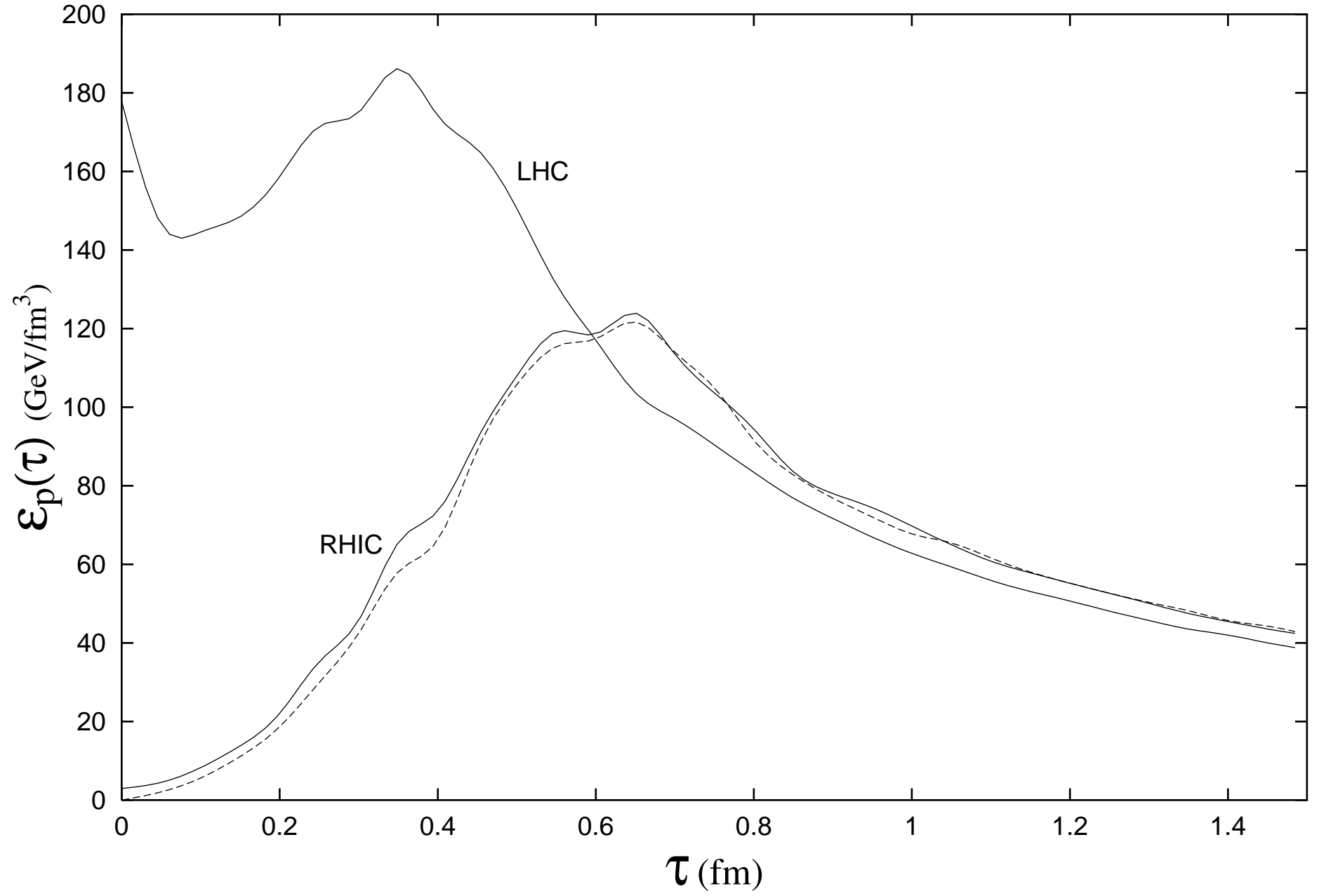


Fig. 2

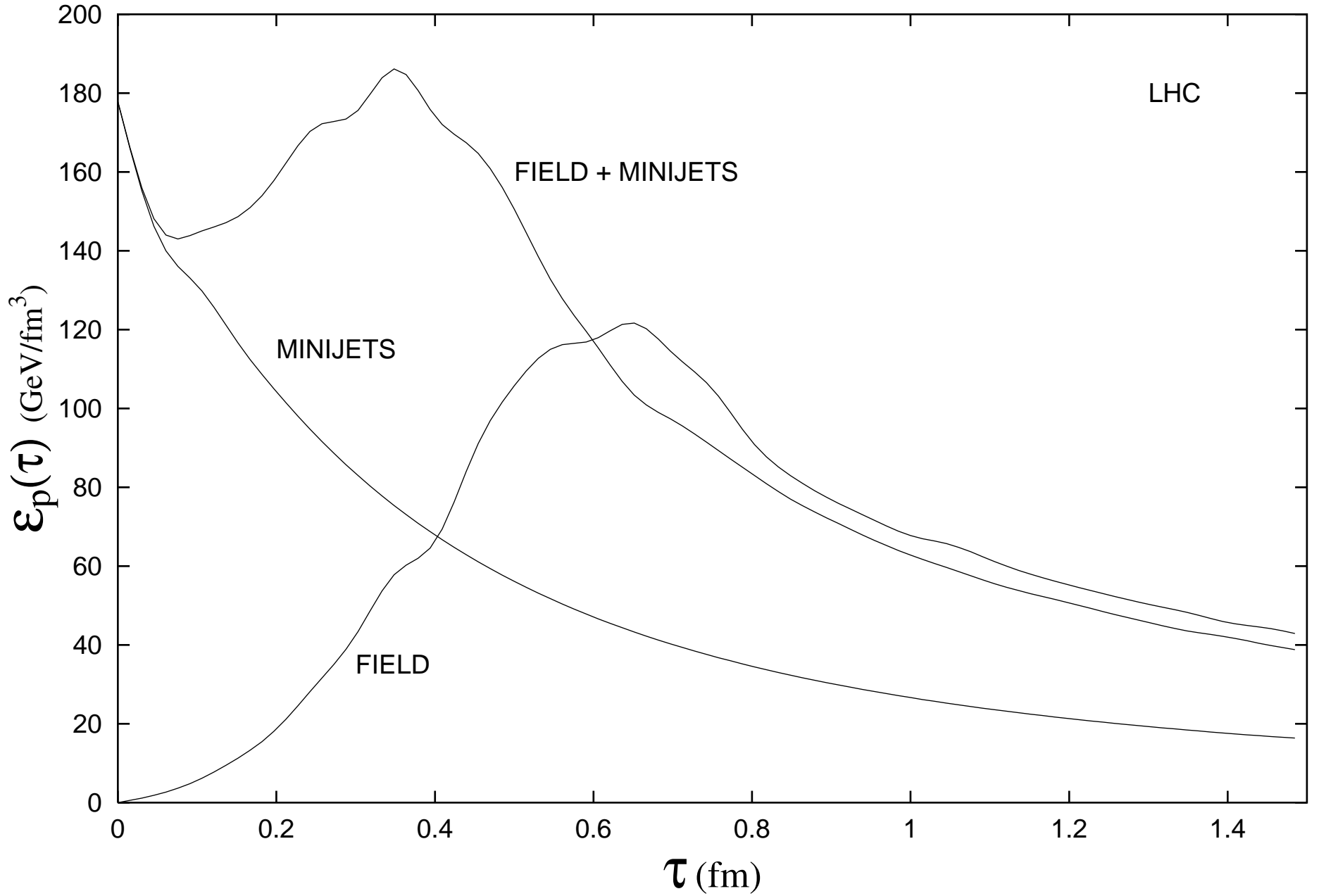


Fig. 3

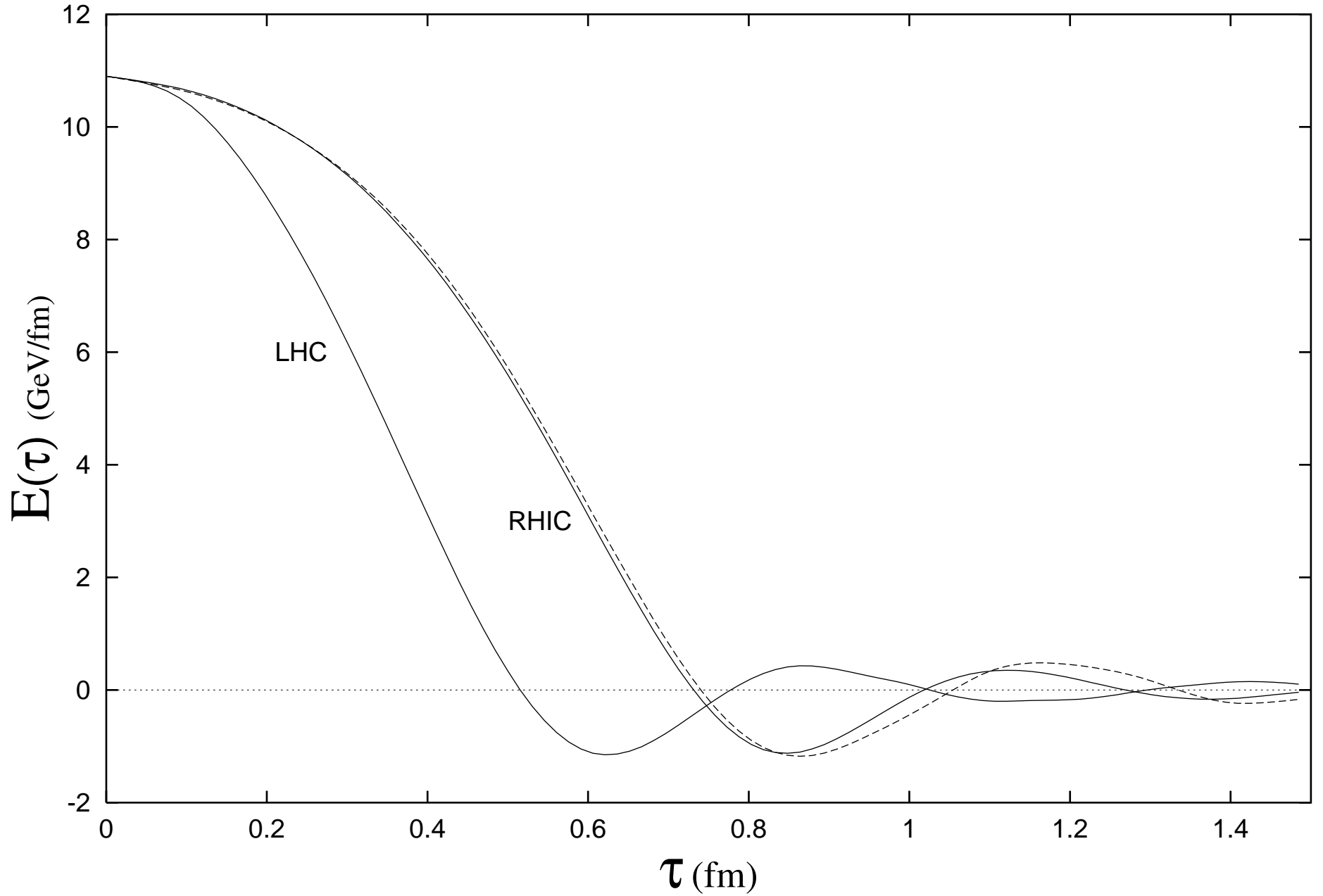


Fig. 4

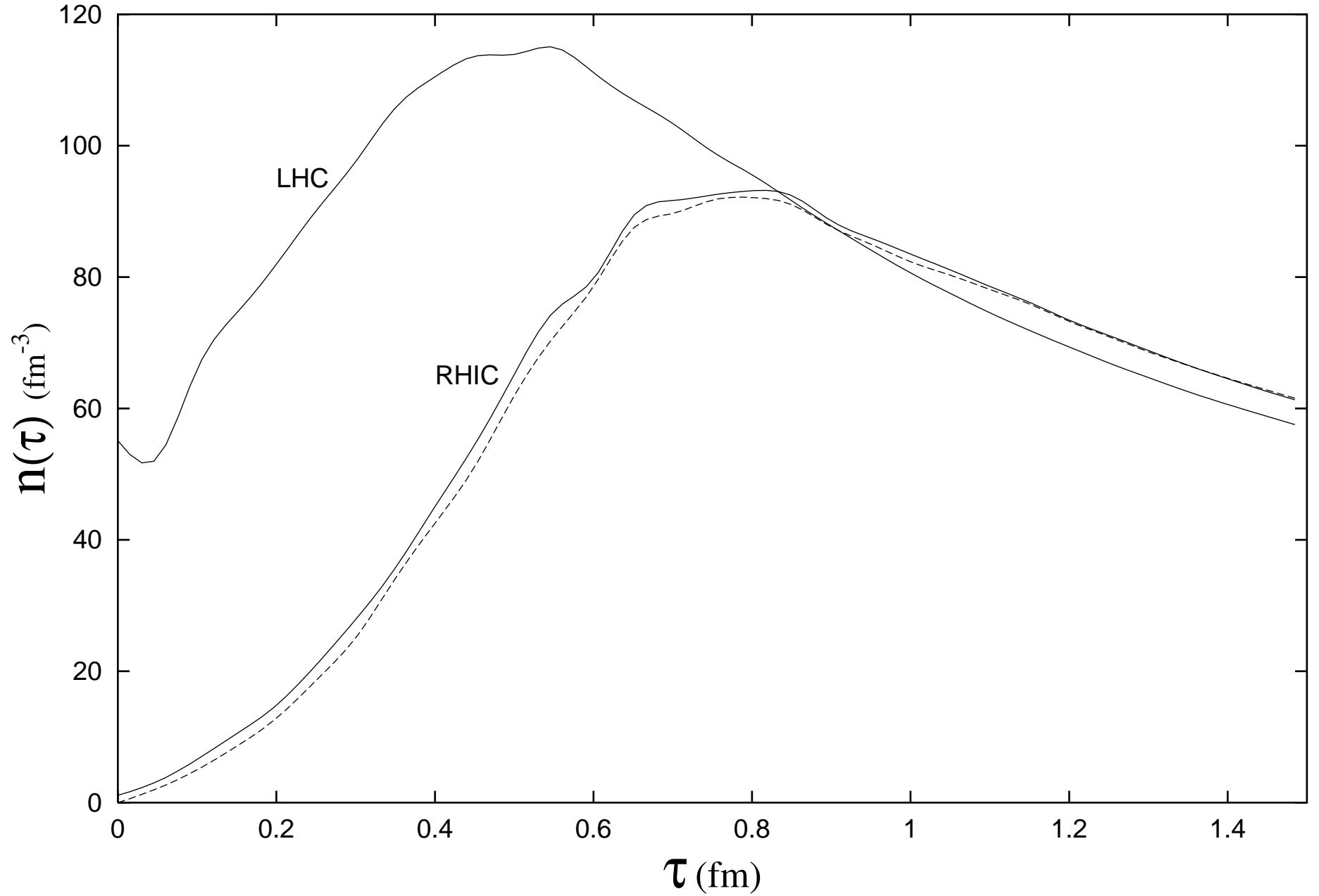


Fig. 5

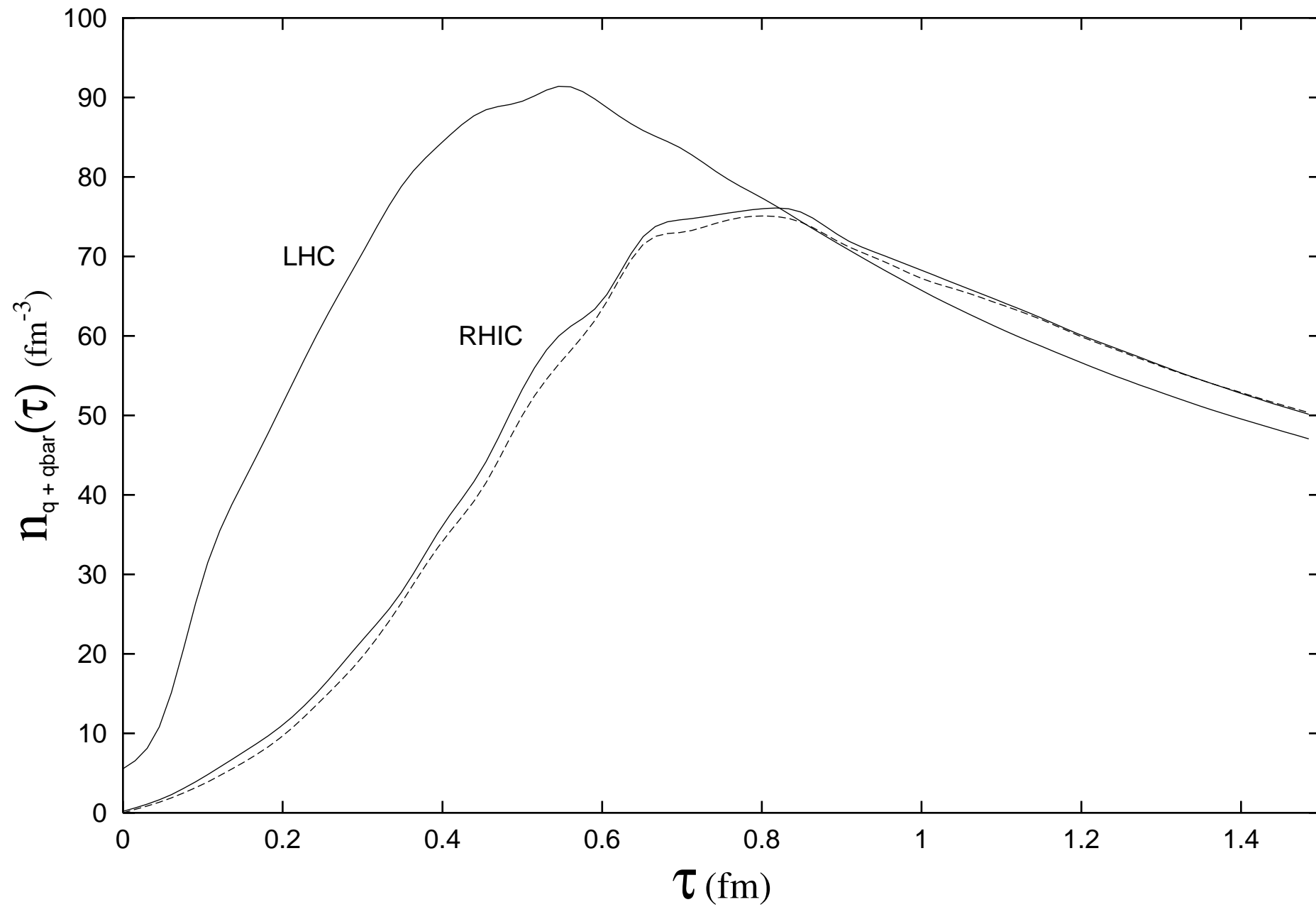


Fig. 6

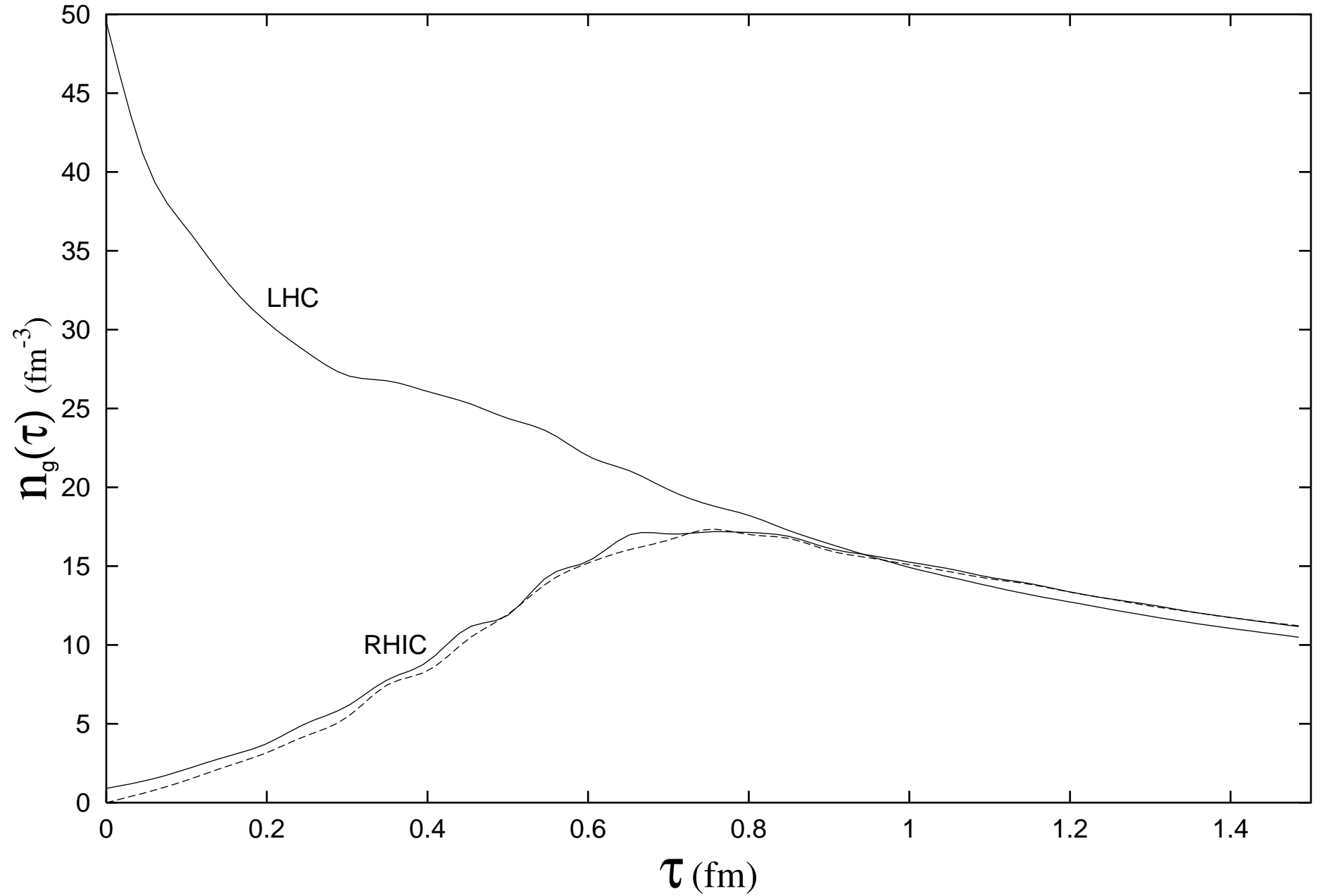


Fig. 7

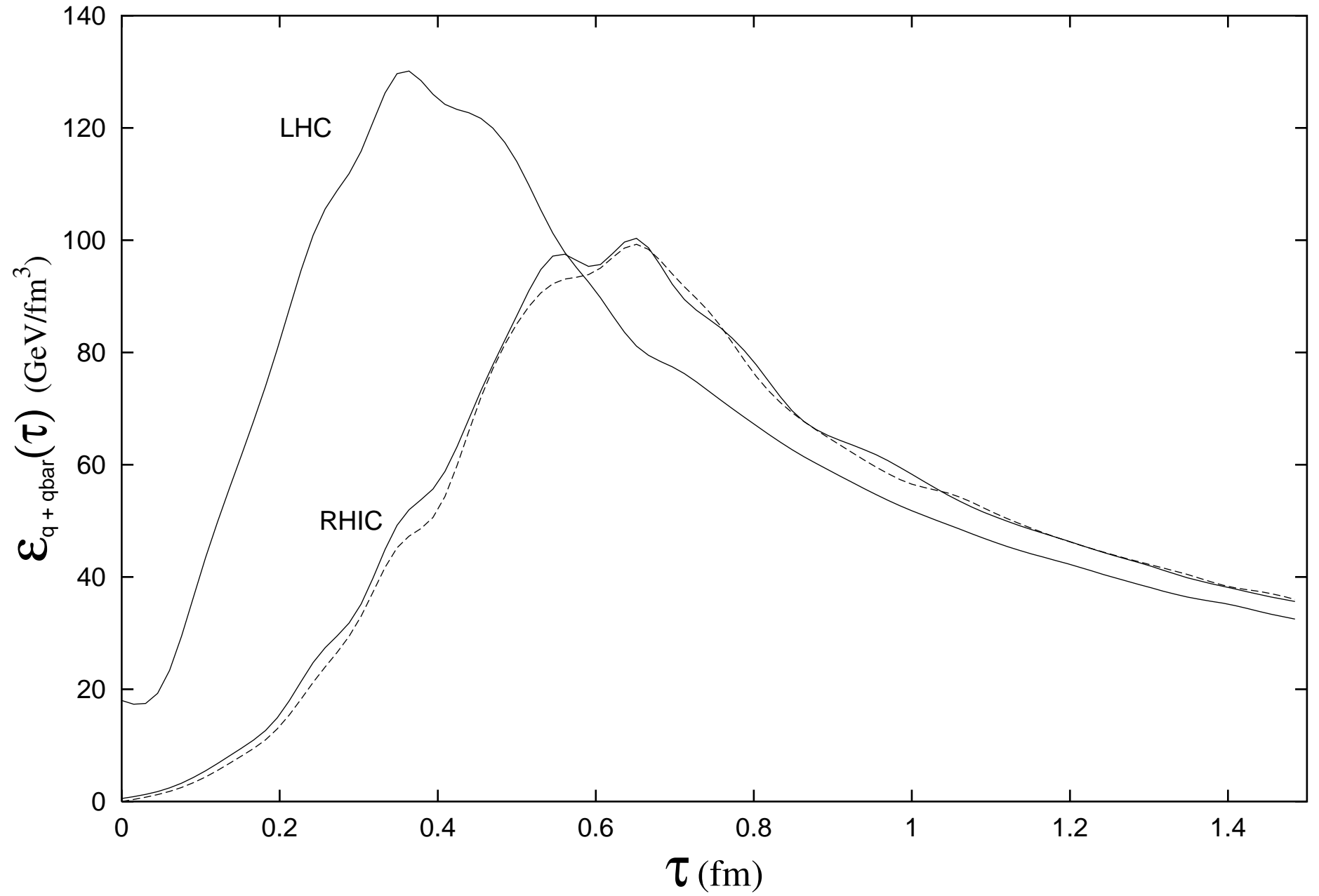


Fig. 8

